International Journal of Electrical and Power Engineering 5 (1): 42-48, 2011
ISSN: 1990-7958

Sensorless Control Strategy for Wind Energy Conversion System Based on Cascaded Doubly Fed Induction Generator Using Artificial Neuronal Network

S. Nouali and A. Ouali
Department of Electrical Engineering, National School of Engineering,
Advanced Control and Energy Management Research Unit,
University of Sfax, Sfax, Tunisia

Abstract: In this study, we present a new sensorless control for Wind Energy Conversion System (WECS) based on Cascaded Doubly Fed Induction Generator (CDFIG). The aim of this control is to extract the maximum wind power and to control the power generation only by measuring phase voltages and currents. The proposed control scheme is ensured without the need of using any rotor speed or wind sensors from the aspect of reliability and increase in cost. For that a neuronal observer is introduced to estimate the rotor speed. To impose the Maximum Power Point (MPPT) an extended luenberger observer was introduced in cascade with the neuronal observer to estimate the optimal aerodynamic torque. After an approximation with an another artificial neuronal network, observer makes it possible to estimate the wind velocity. This later will be injected in the algorithm control to impose the MPPT. Simulation results demonstrate the sensorless control device excellent performances.

Key words: Sensorless control, MPPT, WECS, CDFIG, artificial neuronal network observer, extended luenberger observer

INTRODUCTION

Various types of aero-generators are spread out in the world. The Cascade Doubly Fed Induction Generator (CDFIG) is introduced because it arises as an alternative to the Doubly Fed induction Generator (DFIG) and the Permanent Magnet Synchronous Generator (PMSG). The CDFIG is composed of two doubly fed induction machines called Power Machine (PM) and Control Machine (CM). They are used with the rotors mechanically and electrically coupled.

The great advantages of the CDFIG are the low maintenance requirement avoiding the use of slip ring and brushes and the possibility of reducing or even eliminating the gearbox (Patin *et al*., 2009; Adamowicz *et al*., 2009; Adamowicz and Strzelecki, 2008; Basic *et al*., 2002, 2003; Boardman *et al*., 2002). In addition, the power flow in the power machine can be controlled via a fractionally power converter connected to the control machine stator (Boardman *et al*., 2002; Basic *et al*., 2002).

For that CDFIG have been proposed to apply in new renewable energy generation systems, i.e., small hydropower plants, variable speed windmills, shaft generators of vessels and embedded applications (Patin *et al*., 2009; Adamowicz *et al*., 2009; Adamowicz and Strzelecki, 2008; Basic *et al*., 2002). As all variable-speed constant-frequency generators, we can applied one of the sensorless vector controls to the CDFIG to maximise the system efficiency and to eliminate the rotor speed sensor. In literature, many techniques have been developed for sensorless control for induction machine, PMSG and DFIG applications. The most effective sensorless control techniques are MRAS (Schauder, 1992; Brahmi *et al*., 2009; Cardenas *et al*., 2004), the luenberger observer (Senjyua *et al*., 2006), neuronal network observer (Rahman and Hoque, 1998; Hui *et al*., 2005; Batzel and Lee, 2003; Rajaji and Kumar, 2009; Qiao *et al*, 2009; Barambones *et al*., 2010) and a sliding mode observer (Paponpen and Konghirun, 2007). In this study, we propose a new sensorless control stategy of CDFIG wind turbines based on ANN.

The rotor speed and wind velocity are estimated from the measurement of the power machine currents and grid voltages. The estimated quantities are used then to determine the optimal output power reference by using an MPPT block, based on knowledge of the WECS dynamics and power characteristics for controlling

Corresponding Author: S. Nouali, Department of Electrical Engineering, National School of Engineering,
Advanced Control and Energy Management Research Unit, , University of Sfax, Sfax, Tunisia

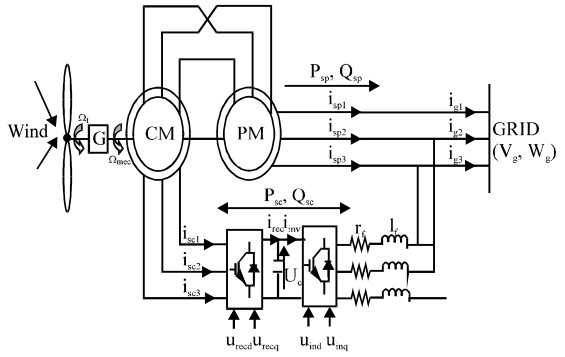

Fig. 1: WECS composition

the CDFIG wind turbine. Consequently, the WECS is optimally controlled to extract the maximum wind power without the need of using any rotor speed or wind sensors. The WECS under study is shown in Fig. 1. It is based on a CDFIG where the power machine stator is directly connected to the power system grid and the control machine stator is connected to a PWM rectifier; allowing an optimal power extraction by the use of an MPPT algorithm. A PWM inverter ensures the injection of the produced power to the AC grid. Between the two converters, a capacitor is used as a voltage DC bus. This system is connected to the grid via a filter to reduce the higher-frequency components.

MATERIALS AND METHODS

Wind turbine modelling: The wind power acting on the swept area of the blade S is a function of the air density ρ and the wind velocity w. The transmitted power P is generally deduced from the wind power using the power coefficient C_p:

$$P = \frac{1}{2} C_p \rho \pi R^2 w^3 \quad (1)$$

The power coefficient is a non-linear function of the tip speed-ratio λ which depends on the wind velocity and the rotation speed of the shaft Ω_t:

$$\lambda = \frac{\Omega_t R}{w} \quad (2)$$

where, R is the blade radius (m). There is a value of $\lambda = \lambda_{opt}$ for which C_p is maximized where the wind turbine captures the maximum wind power. The aerodynamic torque is given by:

$$T_w = \frac{P}{\Omega_t \eta} = \frac{1}{2} C_p \rho \pi R^2 \frac{w^3}{\Omega_t} \quad (3)$$

where, η is the gear ratio. For each wind speed, there exists a specific point in the wind generator power characteristic called Maximum Power Point (MPPT) where the output power is maximized.

CDFIG modelling: The model of the CDFIG can be derived from the models of two DFIG connected as shown in Fig. 1. To obtain the state model of the CDFIG, we adopt the hypotheses of the oriented constant power machine stator flux and we neglect the power machine stator resistor then we have:

$$\phi_{spq} = 0, \frac{d}{dt}\phi_{spd} = 0, v_{gd} = 0$$

And:

$$v_{gq} = \omega_g \phi_{spd} = -V_g$$

Where:

$$\phi_{spd} = \psi_{spd} + l i_{spd}, \phi_{spq} = \psi_{spq} + l i_{spq}$$

Where:

v_{gd} and v_{gq} = d and q components of the grid voltage, respectively
ψ_{spd} and ψ_{spq} = d and q components of the power machine stator flux, respectively
l and V_g = Grid inductance and voltage magnitude, respectively

The CDFIG model placed in (d, q) reference frame which is synchronized with the power machine stator flux rotates at the angular speed $\omega_p = \omega_g$ can be written as:

$$V_{scd} = r_{sc} i_{scd} + \frac{d}{dt}\psi_{scd} - (\omega_g - (p_p + p_c)\Omega_{mec})\psi_{scq} \quad (4)$$

$$V_{scq} = r_{sc} i_{scq} + \frac{d}{dt}\psi_{scq} + (\omega_g - (p_p + p_c)\Omega_{mec})\psi_{scd} \quad (5)$$

Where:

v_{scd} and v_{scq} = d and q components of the control machine stator voltage, respectively
i_{scd} and i_{scq} = d and q components of the control machine stator current, respectively
ω_g = Synchronous pulsation
Ω_{mec} = Aero generator speed
p_p and p_c = Power and control machine pole pairs, respectively
r_{sc} = Control machine stator resistor

Let:

$$k_l = \frac{l_{mc} l_{mp}}{l_{sp} l_r}, l_r = l_r - \frac{l_{mp}^2}{l_{sp}}, l_r = l_{rp} + l_{rc}, l_{sc} = l_{sc} + \frac{l_{mc}^2}{l_r}$$

The control machine stator fluxes are given by the following equations:

$$\psi_{scd} = l_{sc} i_{scd} + k_l \phi_{spd} \quad (6)$$

$$\psi_{scq} = l_{sc} i_{scq} \quad (7)$$

where, l_{sc}, l_{mc} and l_{rc} are the control machine stator, mutual and rotor inductance, respectively; l_{sp}, l_{mp} and l_{rp} are the power machine stator, mutual and rotor inductance, respectively with arrangement of Eq. 4-7 and the CDFIG model can be written under the following form:

$$V_{scd} = r_{sc} i_{scd} + l_{sc} \frac{d}{dt} i_{scd} - l_{sc} (\omega_g - (p_p + p_c)\Omega_{mec}) i_{scq} \quad (8)$$

$$V_{scq} = r_{sc} i_{scq} + l_{sc} \frac{d}{dt} i_{scq} + l_{sc} (\omega_g - (p_p + p_c)\Omega_{mec}) i_{scd} + e_\phi \quad (9)$$

Where:

$$e_\phi = k_l(\omega_g - (p_p + p_c)\Omega_{mec})\phi_{spd}$$

The mechanical equation is given by the following equation:

$$j \frac{d\Omega_{mec}}{dt} = T_w - T_{em} \quad (10)$$

where, T_{em} is the electromechanical torque given by:

$$T_{em} = k_l (p_p + p_c)\phi_{spd} \quad (11)$$

and j is the total inertia which appears on the shaft of the generator (kg m^2).

Converters modelling: The converters are modelled in the d-q reference frame according to the switching function concept (Brahmi *et al*., 2009). The rectifier provides the voltages $V_{scn} = [v_{scd}\ v_{scq}]^T$ from the capacitor voltage U_c and the modulated current r_{ec}:

$$\begin{pmatrix} v_{scd} \\ v_{scq} \end{pmatrix} = \frac{U_c}{2} \begin{pmatrix} u_{recd} \\ u_{recq} \end{pmatrix} \quad (12)$$

$$i_{rec} = \frac{1}{2}(u_{recd} i_{scd} + u_{recq} i_{scq}) \quad (13)$$

where, u_{recd}, u_{recq} are the rectifier modulation functions. The inverter yields, the inverter voltages:

$$V_{invn} = [v_{invd}\ v_{invq}]^T$$

from the capacitor voltage and the inverter modulated current i_{inv} from the line currents $I_{fn} = [i_{fd}\ i_{fq}]^T$:

$$\begin{pmatrix} v_{invd} \\ v_{invq} \end{pmatrix} = \frac{U_c}{2} \begin{pmatrix} u_{invd} \\ r_{invq} \end{pmatrix} \quad (14)$$

$$i_{inv} = \frac{1}{2}(u_{invd} i_{fd} + u_{invq} i_{fq}) \quad (15)$$

where, u_{invd}, u_{invq} are the inverter modulation functions. The DC bus voltage is given by the following differential equation:

$$C \frac{d}{dt} U_c = i_{rec} - i_{inv} \quad (16)$$

where, C is the capacitance of the DC bus. It is assumed that the filters reduce the higher-frequency components. In the d-q reference frame, the voltage balance across the filter inductors and resistors is:

$$v_{invd} - v_{gd} = r_f i_{fd} + l_f \frac{d}{dt} i_{fd} - l_f \omega_g i_{fq} \quad (17)$$

$$v_{invq} - v_{gq} = r_f i_{fq} + l_f \frac{d}{dt} i_{fq} - l_f \omega_g i_{fd} \quad (18)$$

Sensorless control strategy: The WECS include the wind turbine; the CDFIG and the rectifier (Fig. 1). The latter is used to control the control machine stator currents. For that a vector control is necessary. Relating to the CDFIG model given by Eq. 8 and 9, the vector control allows fixing the (d - q) control machine stator voltage as follows:

$$\begin{cases} v_{scd} = v_d + e_d \\ v_{scq} = v_q + e_q + e_\phi \end{cases} \quad (19)$$

Where:

$$e_d = -l'_{sc} (\omega_g - (p_p + p_c)\Omega_{mec})\, i_{scq\_ref}$$

$$e_q = l'_{sc} (\omega_g - (p_p + p_c)\Omega_{mec})\, i_{scd\_ref}$$

v_d and v_q are the de-coupled voltages given by:

$$v_d = (k_p + \frac{k_i}{p})(i_{sed\_ref} - i_{scd})$$

$$v_q = (k_p + \frac{k_i}{p})(i_{seq\_ref} - i_{scq})$$

where, k_i, k_p, k_i', k_p' are the regulators parameters and i_{scd_ref} and i_{scq_ref} are the control machine stator currents reference values. This later are provided by an MPPT block , based on knowledge of the WECS dynamics and power characteristics to extract the maximum wind power for

each wind speed. Consequently, the control scheme requires wind velocity and mechanical speed measures. To increase the installation cost and limit the measurements only on the power machine stator size coupled directly to the grid, a sensorless vector control will be considered. Thus, the control machine stator currents and the mechanical speed in the control laws given by Eq. 19 will be substituted by the estimated one provided from a neuronal network observer.

Artificial neuronal network controller: The ability of the Artificial Neuronal Network (ANN) to approximate nonlinear functions is the most significant. With the potential to shorten and generalize the control scheme configuration and model identification task, neural networks are usually used in many control applications (Brunskill, 2010). In literature, many rotor speed estimation methods using artificial neuronal network has been developed for sensorless control for PMSG (Rahman and Hoque, 1998; Batzel and Lee, 2003; Brahmi *et al*., 2009) and for DFIG (Rajaji and Kumar, 2009; Qiao *et al*., 2009; Barambones *et al*., 2010) wind turbine applications. In the proposed algorithm, the rotor speed is estimated by using the grid voltages and currents of the power machine which is connected directly to the grid. The proposed algorithm use three layers Radial Basis Function Network (RBFN). The three layers were the input, output and hidden layers. The proposed ANN is constituted of 4 inputs and a single output. The overall input-output mapping for the RBFN is given by:

$$\hat{\Omega}_{mec} = b + \sum_{j=1}^{h} w_j \exp\left(\frac{\left\|x - C_j\right\|^2}{\sigma_j}\right) \quad (20)$$

where, Ω_{mec} is the output of the RBNF that represents the rotor speed estimated value; $x = [i_{spd}, i_{spq}, v_{gd}, v_{gq}]$ is the input vector; $\sigma_j \in R$ and $C_j \in R^n$ are the width and center of the jth radial basis function in the hidden layer, respectively; w_j and b are the weight and a bias term between the hidden layer and output one. The parameters of the RBFN including the numbers of Radial Basis Function (RBF) units, the RBF width and centers and the output bias term and weights are determined by using a training data set generated from simulation of the complete drive system.

Once trained, the parameters of the RBFN are then fixed for online estimation of the rotor speed. The proposed RBFN used for rotor speed estimation is shown in Fig. 2. In the network, the circles represent the neurons. The input, output and hidden layers in proposed network are composed, respectively by 4, 5 and 1 neurons.

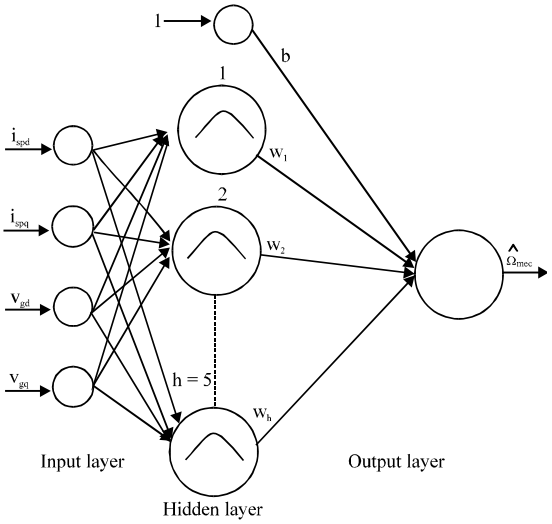

Fig. 2: RBFN-based rotor speed estimation algorithm

Wind velocity and output torque estimation: The maximum point of power MPPT depends on the aerodynamic torque and the wind velocity. From the aspect of reliability and increase in cost, wind velocity sensor is not preferred. To eliminate the latter, wind velocity and output torque estimation techniques may be used.

In some researches, the torque and wind velocity are estimated by an analytical expression deduced from the characteristic curve of the wind turbine aerofoil (Morimoto *et al*., 2005; Senjyua *et al*., 2006). In this study, an extended order luenberger observer was introduced in cascade with the neuronal observer to estimate the optimal aerodynamic torque.

After an approximation with a neuronal network radial basis function makes it possible to estimate the wind velocity. The latter will be injected in the algorithm control to impose the MPPT.

Output torque estimation: By using an extended order luenberger observer, we can extend the estimation to the optimal aerodynamic torque and we can suppose that:

$$\frac{dT_w}{dt} = 0 \quad (21)$$

The luenberger observer is constructed using the CDFIG mechanical Eq. 10 and the optimal aerodynamic torque variation Eq. 21. The observer model is represented by:

$$\begin{cases} \frac{d}{dt}\hat{X}_u = A_u\hat{X}_u + BT_{em} + G(\Omega_{mec} - \hat{\Omega}_{mec}) \\ \hat{\Omega}_{mec} = C_u\hat{X}_u \end{cases} \quad (22)$$

Where:

$$X_u = \begin{bmatrix} \Omega_{mec} \\ T_w \end{bmatrix}, A_u = \begin{bmatrix} 0 & \frac{1}{J} \\ 0 & 0 \end{bmatrix}, B = \begin{bmatrix} -\frac{1}{J} & 0 \end{bmatrix}^T, C_u = \begin{bmatrix} 1 & 0 \end{bmatrix}$$

and G is the matrix gain observer which can written as:

$$G = \begin{bmatrix} g_1 \\ g_2 \end{bmatrix}$$

To ensure the observer stability, we determine the matrix G coefficients so that (A_u - GC_u) is stable. In Eq. 22, T_{em} and Ω_{mec} which are not measurable in the control algorithm are substituted by the estimated values obtained from the neuronal observer.

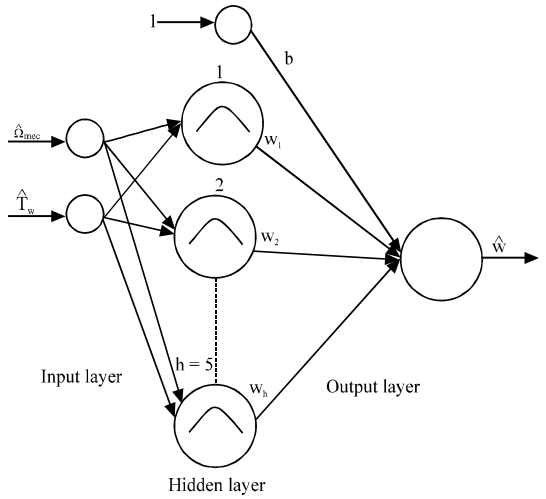

Fig. 3: RBFN-based wind speed estimation algorithm

Wind speed estimation: In the proposed algorithm, the wind speed is estimated by using the estimated aerodynamic torque and rotor speed. We use three layers Radial Basis Function Network (RBFN). As shown in Fig. 3, the network proposed is constituted of 2 inputs corresponding to the estimated aerodynamic torque and rotor speed and a single output corresponding to the estimated wind speed. The latter is used after to impose the optimal output power reference by using an MPPT block, based on knowledge of the WECS dynamics and power characteristics. Figure 4 shows the global sensorless control for wind generation system based on cascade doubly fed induction generator using Artificial Neuronal Network (ANN).

RESULTS AND DISCUSSION

We present the simulation results of the sensorless optimal vector control proposed. The parameters describing the WECS simulated are shown in Table 1. We have considered a real wind speed ranging between 6 and 12 m sec^{-1} with an average value of 9 m sec^{-1} and we chose the unity power factor strategy, i.e., the reactive power injected to the grid via the power machine stator and through the rectifier is set to zero. Figure 5 shows the real and estimated wind speed which is ranged between 6 and 12 m sec^{-1}. Figure 6 shows the estimated rotor speed using the proposed method it was consistent with

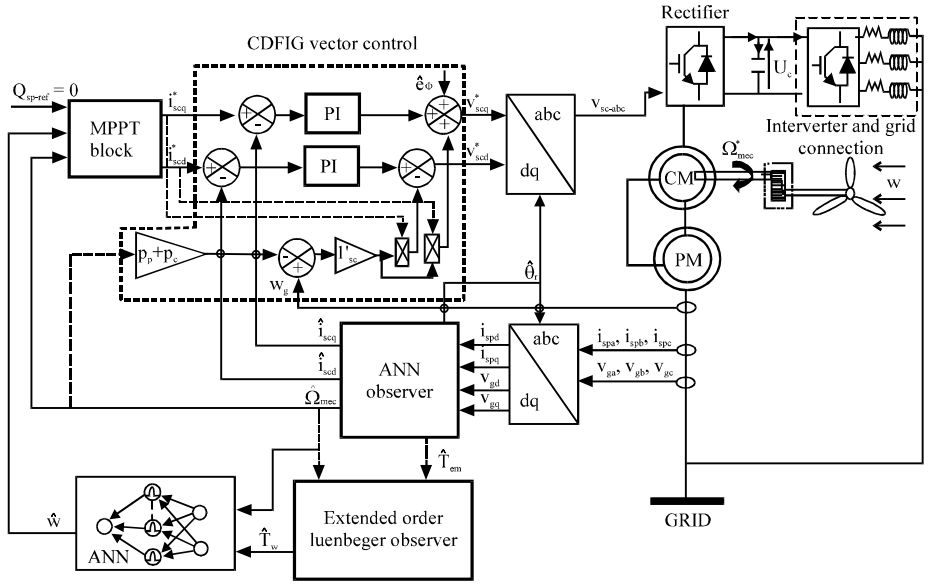

Fig. 4: Block diagram of global sensorlesss control for wind generation system based on CDFIG

Table 1: Characteristics of the WECS simulated

Parameters	Values
l_{sp}	0.0073 H
l_{rp}	0.0061 H
l_{mp}	0.0062 H
r_{rp}	0.0073 Ω
r_{sp}	0 Ω
l_{sc}	0.0073 H
l_{rc}	0.0061 H
l_{mc}	0.0062 H
r_{sc}	0.0073 Ω
r_{rc}	0.0073 Ω
p_p	1
p_c	1
ω_p	100 pi rad
ω_g	100 pi rad
V_g	220 V
r_f	0.0002 Ω
l_f	5 μH
U_c	600 V
C	4400 F
j	4 kg m^2

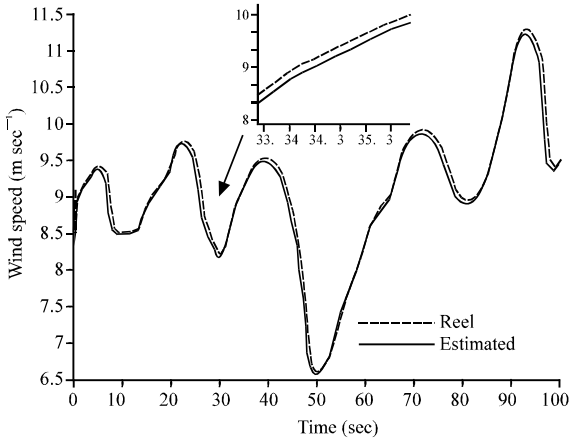

Fig. 5: Wind speed

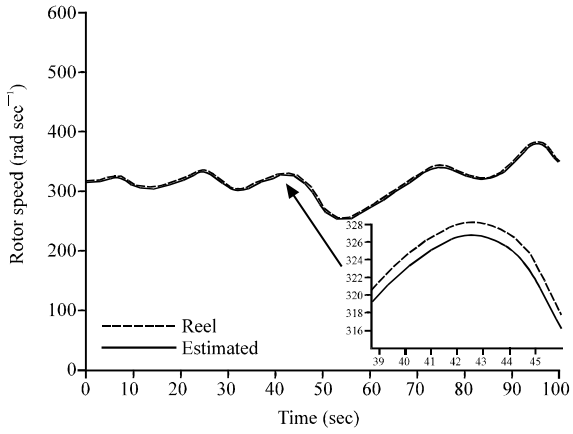

Fig. 6: Rotor speed

real method it was consistent with the real shaft speed. The output torque and the aerodynamic power shown in Fig. 7 and 8, respectively, are also well estimated.

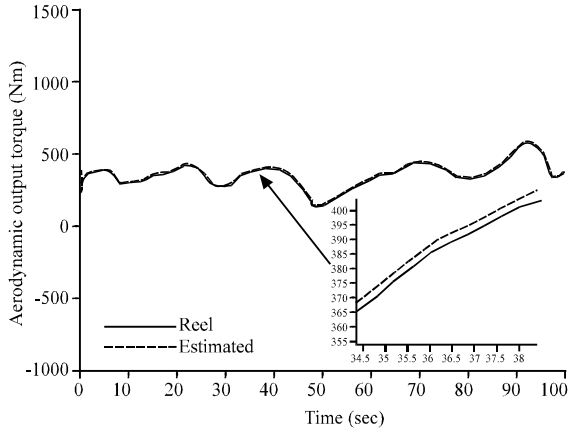

Fig. 7: Output torque of the wind turbine

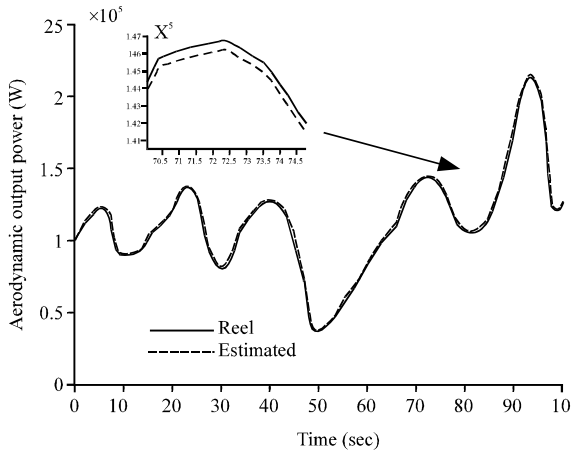

Fig. 8: Aerodynamic output power

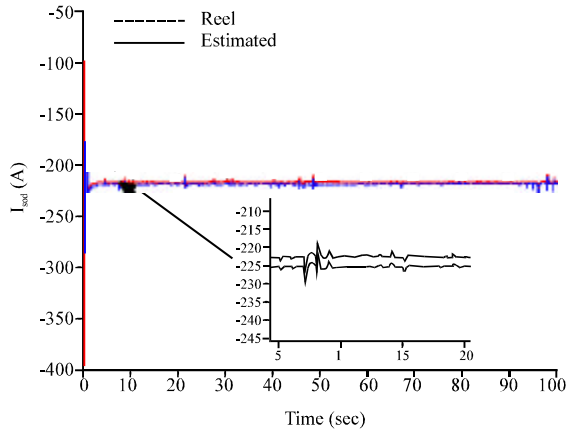

Fig. 9: D-component of the control machine stator current

The d and q control machine stator currents components are given, respectively in Fig. 9 and 10. We note that the currents are correctly estimated during the time.

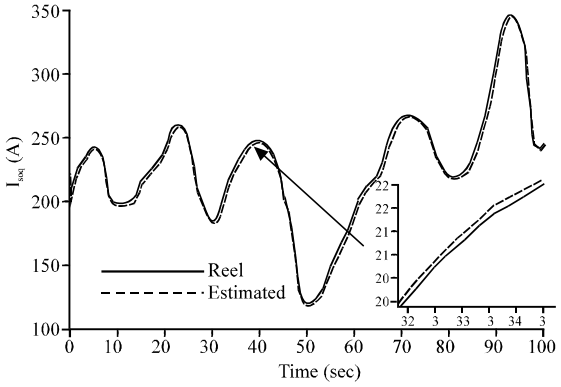

Fig. 10: Q-component of the control machine stator current

CONCLUSION

From the aspect of reliability and increase in cost, a sensorless vector control of a WESC based on ANN was proposed. In the proposed method, a three layers radial basis function network is used for estimating the shaft speed. In addition, an extended luenberger and another neuronal observer were used to estimate the wind velocity to impose the MPPT. Simulation result was illustrated to improve the sensorless control strategy.

REFERENCES

Adamowicz, M. and R. Strzelecki, 2008. Cascaded doubly fed induction generator for mini and micro power plants connected to grid. Proceeding of the 13th International Conference on Power Electronics and Motion Control, Sept. 1-3, Poznan, Poland, pp: 1729-1733.

Adamowicz, M., R. Strzelecki and P. Mysiak, 2009. Cascaded doubly fed induction generator using PFC rectifiers. Proceedings of the International Conference on Compatibility and Power Electronics, May 20-22, Badajoz, Spain, pp: 186-190.

Barambones, O., J.M.G. Durana and E.Kremers, 2010. A neural network based wind speed estimator for a wind turbine control. Proceeding of the MELECON the 15th IEEE Mediterranean Electrotechnical Conference, April 26-28, Valletta, pp: 1383-1388.

Basic, D., J.G. Zhu and G. Boardman, 2002. Modeling and steady-state performance analysis of a brushless doubly fed twin stator induction generator. Melbourne Australia.

Basic, D., J. Zhu and G. Boardman, 2003. Transient performance study of a brushless doubly fed twin stator induction generator. IEEE Trans. Energy Convers., 18: 400-408.

Batzel, T. and K.Y. Lee, 2003. An approach to sensorless operation of the permanent-magnet synchronous motor using diagonally recurrent neural networks. IEEE Trans. Energy Convers., 18: 100-106.

Boardman, G., J.G. Zhu and Q.P. Ha, 2002. General reference frame modelling of the doubly fed twin stator induction machine using space vectors. Melbourne Australia.

Brahmi, J., L. Krichen and A. Ouali, 2009. Acomparative study between three sensorless control strategies for PMSG in wind conversion system. Appllied Energy, 89: 1565-1573.

Brunskill, A.W., 2010. A neural network-based wake model for small wind turbine siting near obstacles. Ph.D. Thesis, University of Guelph.

Cardenas, R., R. Pena, J. Proboste, G. Asher and J. Clare, 2004. MRAS observer for sensorless control of standalone doubly fed induction generators. IEEE Trans. Energy Convers., 19: 710-718.

Hui, L., K.L. Shi and P.G. McLaren, 2005. Neural-network-based sensorless maximum wind energy capture with compensated power coefficient. IEEE Trans. Indus. Appl., 41: 1548-1556.

Morimoto, S., H. Nakayama, M. Sanada and Y. Takeda, 2005. Sensorless, output maximization control for variable-speed wind generation system using IPMSG. IEEE Trans. Indus. Appl., 4: 60-67.

Paponpen, K. and M. Konghirun, 2007. Speed sensorless control of PMSM using an improved sliding mode observer with sigmoid function. ECTI Trans. Electr. Eng. Electron. Commun., 5: 51-55.

Patin, N., E. Monmasson and J.E. Louis, 2009. Modeling and control of a cascaded doubly fed induction generator dedicated to isolated grids. IEEE Trans. Indus. Electron., 56: 4207-4219.

Qiao, W., X. Gong and L. Qu, 2009. Output maximization control for DFIG wind turbines without using wind and shaft speed measurements. IEEE Energy Convers. Cong. Exposit.

Rahman, M.A. and M.A. Hoque, 1998. On line adaptive artificial neural network based vector control of permanent synchronous motors. IEEE Trans. Energy Convers., 13: 311-318.

Rajaji, L. and C. Kumar, 2009. Neural network controller based induction generator for wind turbine applications. India. J. Sci. Technol., 2: 70-74.

Schauder, C., 1992. Adaptive speed identification for vector control of induction motors without rotational transducers. IEEE Trans. Ind. Appl., 28: 1054-1061.

Senjyua, T., S. Tamakia, E. Muhandoa, N. Urasakia and H. Kinjoa *et al*., 2006. Wind velocity and rotor position sensorless maximum power point tracking control for wind eneration system. Renewable Energy, 31: 1764-1775.